

Granular solids transmit stress as two-phase compositesRaphael Blumenfeld ^{*}*Gonville & Caius College, University of Cambridge, Trinity St., Cambridge CB2 1TA, United Kingdom*

(Received 4 September 2023; accepted 29 November 2023; published xxxxxxxxx)

A basic problem in the science of realistic granular matter is the plethora of heuristic models of the stress field in the absence of a first-principles theory. Such a theory is formulated here, based on the idea that static granular assemblies can be regarded as two-phase composites. A thought experiment is described, demonstrating that the state of such materials can be varied continuously from marginal stability, via a two-phase granular assembly, then porous structure, and finally be made perfectly elastic. For completeness, I review briefly the condition for marginal stability in infinitely large assemblies. The general solution for the stress equations in $d = 2$ is reviewed in detail and shown to be consistent with the two-phase idea. A method for identifying the phases of finite regions in larger systems is constructed, providing a stability parameter that quantifies the “proximity” to the marginally stable state. The difficulty involved in deriving stress fields in such composites is a unique constraint on the boundary between phases, and, to highlight it, a simple case of a stack of plates of alternating phase is solved explicitly. An effective medium approximation, which satisfies this constraint, is then developed and analyzed in detail. This approach forms a basis for the extension of the stress theory to general granular solids that are not marginally stable or at the yield threshold.

DOI: [10.1103/PhysRevE.00.004900](https://doi.org/10.1103/PhysRevE.00.004900)**I. INTRODUCTION**

Granular matter (GM), whose ubiquity on Earth is second only to water, is essential not only to human society but also to most life on land. It is often regarded as a distinct form of matter because of its rich behavior, which is dissimilar from the conventional forms of matter. Of essential importance is understanding and predicting how GM transmits stress. A first-principles stress theory in these materials is essential in a wide range of disciplines: civil, structural, and chemical engineering; geology and earth sciences; and physics, as well as in technological applications of powders, soils, foodstuff, etc. It is also key to mitigation of hazards, from snow and soil avalanches to deflecting rubble-pile asteroids.

The science of GM is at least 2200 years old. Indeed, what is regarded today as the oldest existing scientific publication, dating back to the third century BCE [1], involved GM. To an extent, this is attestation of the significance of this field. In the late 19th century [2] and in the early 20th century [3], work on GM was motivated by practical applications and was mainly done within the context of engineering. The last three decades saw an explosion of fundamental theoretical research, following the seminal work of Edwards [4–6]. Yet, in spite of this uniquely long history and intensified recent research activity,

no first-principles stress theory for such media exists. One of the reasons is that, unlike any conventional continuum, GM behaves as a combination of a solid and a fluid, and it transmits stress very nonuniformly, often via stress chains [7–14]. Another reason is that there is a range of phenomenological and empirical models, utilized in engineering, providing the impression that one can get away without a fundamental theory. This situation is unsatisfactory, and, indeed, subsidence and collapses of buildings and structures provide evidence that, while useful, empirical models have serious limitations.

It has been suggested that one of the hurdles to constructing such a stress theory is that GM is regarded paradigmatically as a continuum endowed with some constitutive properties, for which stress equations need to be developed. Since this approach has not been fruitful for many decades, it was proposed that general GM needs to be regarded rather as two-phase composites, with each phase satisfying different stress field equations [15]. It is this view that I intend to explore in the following.

Specifically, several arguments are presented in support of the two-phase-composite idea, and a simple case of such a composite is solved. A method to derive the stress from first principle in such media, using an effective medium approach, is formulated. To alleviate a difficulty in distinguishing between the different phases visually, which is important for the purpose of imposing boundary conditions on the phase boundaries, a quantitative stability parameter is developed, which can also be used as a phase field parameter. To make this paper self-contained, I also review briefly (1) the method of identifying marginally stable granular assemblies and (2) the current isostaticity stress theory (IST) for the marginally stable state of GM, with a specific solution in two dimensions ($d = 2$).

^{*}rbb11@cam.ac.uk

Published by the American Physical Society under the terms of the Creative Commons Attribution 4.0 International license. Further distribution of this work must maintain attribution to the author(s) and the published article’s title, journal citation, and DOI.

The structure of the paper is the following. In Sec. II the state of marginal stability of GM is defined quantitatively in terms of the particle-scale mean coordination number (MCN). In Sec. III the existing stress theory for marginally stable GM is reviewed briefly, with more details, including the general solution in two-dimensional systems, given in the Supplemental Material [16]. In Sec. IV I discuss the role of the marginally stable state as a critical point in the traditional sense, with a proper diverging response length, which is reflected in the increasing typical length of force chains. This state, which is also the yield threshold, is often referred to as a critical state in the engineering literature, albeit without the connotation that this term usually carries in physics. A thought experiment is then described, which illustrates clearly that GM is a two-phase composite, with one phase isostatic and the other elastic. The larger the concentration of the former phase the longer the response length. In Sec. V the construction of a general stress theory for such two-phase composites is discussed. An example of a simple case, in which alternate-phase plates are arranged in series, is analyzed, solved exactly, and used to illustrate a fundamental difficulty, which can be traced back to the assumptions of isostaticity theory. Then a possible extension by an effective medium method is described, and the difficulties posed by a more general theory are discussed. In Sec. VI a stability parameter is introduced, which makes possible a local quantitative distinction between the phases in finite granular regions. This parameter also enables a quantitative determination of the “distance” from the critical point. Finally, the results and some implications are discussed in the concluding Sec. VII.

II. THE MARGINALLY STABLE STATE

At the macroscopic, many-particle level, the marginally stable state is the (macro-)state at the yield threshold between the fluid and solid states. It is also known as critical, marginally rigid, and isostatic state. The reason that this is the yield threshold can be traced to the particle level, at which the number of force-carrying interparticle contacts is such that the number of equations to determine the interparticle forces is exactly equal to the number of unknown force components that require determination. When there are too few such contacts, the medium is unstable and must rearrange under external forces. This state is marginally stable because any perturbation in the applied load or a particle’s position gives rise to contact breaking and to local rearrangement. This perturbs neighbor particles and so on. Thus, a perturbation of one contact can lead to a rearrangement of a significant portion of the granular assembly. Such a long-range response to a perturbation is the hallmark of a critical point, as will be discussed below.

The difference between the numbers of unknowns and balance equations to determine them is quantified by the mean coordination number (MCN), z , which is defined as the number of force-carrying contacts per particle. The marginally stable state corresponds to a “critical” value, z_c , which depends on the dimensionality, d , whether the particles are frictional or are frictionless, and whether they are perfectly circular, spherical, hyperspherical, or of other shapes. When $z < z_c$, the medium is fluid and when $z > z_c$ it is solid.

To determine z_c , we need to consider d -dimensional many-particle assemblies of N ($\gg 1$) rigid particles of convex shapes. It is straightforward to extend the discussion to some classes of nonconvex shapes and to compliant hard particles, but this would add very little insight and this issue is better circumvented here. In the following analysis, only fixed compressive boundary forces are presumed to act on the granular assemblies—external force fields, including gravity, are ignored. The justification for this is that given a static structure of an assembly, the stress equations discussed below are linear, which means that the effects of an external force field can be superposed on the IST solution.

A. Frictional particles

Frictional particles experience d force components at each contact point, which need to be determined. Neglecting boundary effects for very large assemblies, summing over the coordination numbers around all particles, results in twice the total number of contacts, C_d : $C_d = Nz/2$. There are therefore $dNz/2$ unknowns. To be mechanically stable, each particle must satisfy d conditions of force balance and one torque balance condition for each of the $d(d-1)/2$ axes of rotation. The critical MCN must then satisfy the equality

$$d \frac{z_c}{2} N = \left[d + \frac{d(d-1)}{2} \right] N \Rightarrow z_c = d + 1. \quad (1)$$

This calculation can be found extensively in the literature.

B. Frictionless non-(hyper-)spherical particles

In this case the force must be normal to the tangent plane at the contact point, and, therefore, the geometry determines the direction of any contact force. This leaves only one unknown per contact—the force magnitude. The number of unknowns is then $C_d = z_c N/2$. The number of equations is the same as on the right-hand side of Eq. (1), and equating it with the number of unknowns yields

$$z_c = d(d + 1). \quad (2)$$

C. Frictionless hyperspherical particles

An assembly of frictionless perfect hyperspheres, which includes disks in $d = 2$, is often used in numerical simulations because it is convenient for contact detection and contact force transmission. However, not only is it difficult to reproduce physically, but such an assembly is also degenerate in the sense that balance of forces on every particle ensures automatically balance of torques. Therefore, the torque balance conditions are redundant for all particles, and only the Nd force balance conditions must be satisfied. Since, for such particles, the forces are also normal to the contact tangent plane, there is only one unknown to determine at each of the $z_c N/2$ contact points. Equating unknowns and equations then yields

$$z_c = 2d. \quad (3)$$

It should be commented that the values for z_c , calculated for all types of particles, incur boundary corrections of order

181 $O(N^{-1/d})$, which have been neglected. These corrections will
 182 become relevant for the discussion in Sec. VI.

183 **III. CRITICAL STRESS TRANSMISSION**
 184 **AT MARGINAL STABILITY**

185 As mentioned, force chains are the conduits of stress and
 186 displacement perturbations, and the longer they are the further
 187 the response. In particular, in the marginally stable state the
 188 typical length of force chains is comparable to the system
 189 size, making this state the equivalent of a conventional critical
 190 point. This equivalence is key to understanding stress trans-
 191 mission in more general states of GM. It is therefore useful
 192 to review briefly the theory of stress transmission at marginal
 193 stability.

194 Any continuum stress theory must satisfy the balance con-
 195 ditions:

$$\vec{\nabla} \cdot \overline{\overline{\sigma}} = \vec{g}_{\text{ext}} \quad (\text{balance of forces}) \quad (4)$$

$$\overline{\overline{\sigma}} = \overline{\overline{\sigma}}^T \quad (\text{balance of torques}). \quad (5)$$

196 In d dimensions, the first equation provides d conditions,
 197 the second $d(d-1)/2$, and together $d(d+1)/2$ conditions
 198 in total. Since the stress tensor has d^2 components, further
 199 $d(d-1)/2$ equations are required to determine it. These “clo-
 200 sure” equations need to be provided by constitutive relations.
 201 In elasticity theory, the closure is by St. Venant’s compatibility
 202 constraints on the strain tensor, augmented with stress-strain
 203 relations [17]. Such closure, however, is not appropriate for
 204 the marginally stable state. This is because the stress field is
 205 nothing but a continuum representation of the spatial distribu-
 206 tion of interparticle forces in the marginally stable state, and,
 207 since these forces are exactly determinable by the structure
 208 and are independent of any infinitesimal displacement that led
 209 to it, then the continuum stress cannot depend on the strain
 210 field. This is also evident from the fact that no elastic moduli
 211 are involved in the above discussion of the determination
 212 of those forces. It follows that the only relevant constitutive
 213 characteristics must be based on the local structure. The ob-
 214 servations of nonuniform stress transmission in GM via chains
 215 [7–14] further supports the idea that the equations cannot be
 216 elliptic and therefore cannot arise from strain-based constitu-
 217 tive relations. It was proposed then that the closure is by a
 218 stress-structure relation [18–21],

$$\overline{\overline{M}} : \overline{\overline{\sigma}} = 0, \quad (6)$$

219 in which $\overline{\overline{M}}$ is a symmetric tensor that characterizes the lo-
 220 cal structure. Its determinant is negative, which results in
 221 *hyperbolic* equations, in contrast to the elliptic equations of
 222 elasticity theory. This gives rise to solutions that “propagate”
 223 into the medium along characteristic paths. Along these paths,
 224 which can be interpreted as stress chains, characteristic stress
 225 combinations are constant. The set of equations (5) and (6)
 226 are commonly called *isostaticity theory*. So far, the tensor $\overline{\overline{M}}$
 227 has been derived from first principles only in $d = 2$ [15,22–
 228 24]. Nevertheless, there is a range of empirical models for it,
 229 or leading to it, in $d = 2$ and 3, e.g., Mohr-Coulomb [25],
 230 Tresca [26], von Mises [27], and Drucker and Prager [28].
 231 The characteristics can be straight or curved and even bend

backwards [24]. A brief outline of the solution of these equa-
 tions in rectangular coordinates and an example of a solution
 are given in the Supplemental Material [16]. It should be
 commented that the first-principles theory holds for compliant
 particles, as long as the MCN is z_c and the compressed areas at
 contacts are small compared to the particle sizes. Compliance
 introduces corrections to the solutions of Eqs. (5) and (6),
 which decay as the number of particles increases [29].

The marginally stable state acts as a critical point in that
 a small displacement of a particle can lead to the yield of
 large part of the assembly [14,30–32]. The main descriptor
 of this state is the critical MCN, z_c , and the deviation from
 this state can be parameterized by the difference $z - z_c$. The
 critical nature of the marginally stable state opens the door
 to modeling GM in general, which is the subject of the next
 section.

It should be commented in passing that, while it is tempting
 to consider the typical length of the characteristic stress chains
 as a descriptor of the long-range correlation, this similarity
 holds only for uniform fabric tensors, $\overline{\overline{M}}$. This is because
 stress chains straight in such systems and span the entire
 system. However, when $\overline{\overline{M}}$ is nonuniform, the stress along
 the characteristics decays with distance and so do the effects
 of local perturbations. There is some fundamental difference
 between the force chains, observed in experiments with pho-
 toelastic particles [11,33–37], and stress chains. The former
 are observed only when above some threshold, and, therefore,
 the definition of a force chain is not sharp to some extent.
 In contrast, theoretical stress chains are defined uniquely and
 unambiguously, given the fabric tensor $\overline{\overline{M}}$.

IV. GENERAL GM IS A TWO-PHASE COMPOSITE

While isostaticity is an established first-principles theory,
 marginally stable states are rare in realistic static systems, re-
 quiring specialized dynamics to generate them. The MCNs of
 most solid granular assemblies, whether natural or manmade,
 often exceed z_c . The question is how to extend the isostaticity
 stress theory to such media. To this end, it has been proposed
 that, at least sufficiently close to the marginally stable state,
 realistic GM must be regarded as composites comprising re-
 gions of two phases: one is marginally stable and the other
 is overconnected, in which $z > z_c$ [15]. The usefulness of
 the *two-phase composites* picture can be illustrated with the
 following thought experiment.

Consider a large assembly of elastic particles, e.g., rub-
 ber balls, initially at a marginally stable state under some
 infinitesimally small boundary forces. Under such loading,
 the contact areas can be made much smaller than the small-
 est ball diameter, and isostaticity theory provides the correct
 solution for the stress field. Now, increase all the boundary
 forces uniformly by a factor $\alpha = 1 + \epsilon$, with $0 < \epsilon$. When ϵ
 is sufficiently small, such that it cannot bring even the closest
 pair of particles into contact, the number of contacts remains
 the same, and only their areas increase as they are compressed
 slightly. In a very large assembly, this has been shown only
 to introduce small corrections to the original solution, with
 the corrections decaying with system size. As ϵ increases,
 new contacts are made here and there, and the MCN starts
 to increase: $z = z_c + \delta z$. When $\delta z \ll 1$, the overconnected

290 regions are small and isolated. A force chain incident on such
 291 a region “scatters” in the sense that its continuation is shared
 292 by more contacts than required for marginal stability. This
 293 sharing means that each of the forces emerging from this
 294 region is lower in magnitude. Setting the magnitude obser-
 295 vation threshold of force chains appropriately, the incident
 296 force chain effectively “terminates.” As α increases, more
 297 overconnected regions form, the typical length of force chains
 298 decreases, and with it the stress. This resembles strongly the
 299 behavior of traditional systems as they move away gradually
 300 from critical points. For example, increasing the temperature
 301 slightly above the critical point introduces regions of normal
 302 conductivity, or increasing the concentration of nonconduct-
 303 ing elements at the percolation threshold through an otherwise
 304 conducting system reduces the conductivity by generating
 305 nonconducting regions.

306 Another effect of increasing α is that contact areas between
 307 particles in contact increases. When the size of such a contact
 308 becomes comparable to the size of either of the particles
 309 sharing it, this pair can no longer be regarded as two sepa-
 310 rate particles. As balls get squeezed together and the contact
 311 areas of sufficiently many reach this limit, the assembly can
 312 no longer be regarded as granular and is, rather, a porous
 313 medium, comprising an elastic solid phase and cavities or
 314 pores. Some models for computing stress transmission in this
 315 type of media exist [38,39], but discussing them is tangential
 316 to this presentation. Finally, at some large value of α , these
 317 voids are also squeezed out completely, and the system be-
 318 comes a continuous uniform elastic solid. The stress fields in
 319 such a solids are readily calculated by conventional elasticity
 320 theory.

321 This thought experiment shows that there is a continuous
 322 spectrum of structures with the marginally stable critical point
 323 at one end and a perfectly elastic state at the other. General
 324 GM is on this spectrum sufficiently close to the former, before
 325 the appearance of porous media. In particular, where on this
 326 spectrum a granular solid exactly is depends on the difference
 327 $\delta z = z - z_c$, which is tantamount to saying that it depends on
 328 the response length.

329 It is clear that, in assemblies of particles that are not as elas-
 330 tic as rubber balls, other physical mechanisms may intervene
 331 before the porous medium state or the continuum are reached,
 332 such as particle fragmentation, phase transitions, etc. These
 333 are all ignored because they are irrelevant to the purpose of
 334 this thought experiment. Additionally, if the original particu-
 335 lates are made of nonelastic materials, the stress transmission
 336 in the final continuous phase need not satisfy the equations of
 337 elasticity theory. All these side issues notwithstanding, start-
 338 ing from a perfectly elastic final state is a useful first step
 339 toward a more general theory. The two-phase idea may also
 340 provide insight into the observation of two distinct sets of
 341 force chain networks in simulations of GM [40]. In any case,
 342 this conceptual picture suggests a strategy to extend the theory
 343 beyond the ideal marginally stable limit, and this strategy is
 344 discussed next.

345 **V. TOWARD A CONTINUUM STRESS THEORY**
 346 **OF GENERAL GM**

347 Field theories of two-phase composites are generally diffi-
 348 cult to construct except when the phases have a special spatial

349 distribution. The main existing methods for arbitrary spatial
 350 distributions are effective medium approximation, mean field
 351 theory, and renormalization near critical points. Each of these
 352 methods involves some special assumptions. Unfortunately,
 353 none of these models can be applied directly to GM com-
 354 posites because they are based on the assumption that the
 355 two phases satisfy the same field equations and they differ
 356 only by their constitutive properties. Example are mixtures of
 357 two conducting materials, in which both phases obey Ohm’s
 358 law, but have different conductivities; composites of elastic
 359 materials, which are often presumed to obey the same stress
 360 equations but with different elastic moduli; and mixtures of
 361 dielectrics having electric-displacement fields relation of the
 362 same functional form, but with different dielectric constants.
 363 The two-phase GM problem is more difficult because the
 364 phases differ not by their constitutive properties but by the
 365 stress equations that they satisfy. This problem is exacerbated
 366 by the fact that the elastic phase satisfies elliptic equations
 367 and the marginally stable phase satisfies hyperbolic equations.
 368 While the former can be solved under Dirichlet boundary
 369 conditions, the latter can be ill-posed under such conditions.
 370 Thus, much care is required even in posing the problem.

371 **A. Isostatic-elastic pair of plates**

372 To illustrate the complexity of the problem, it is useful
 373 to start with a simple solvable structure in two dimensions.
 374 Consider only the two parallel plates, **I** and **II**, sketched in
 375 Fig. 1. Plate **I** is isostatic, occupying $0 < x < W_1$ and $-\infty <$
 376 $y < \infty$, and plate **II** is elastic, occupying $W_1 < x < W_2$ and
 377 $-\infty < y < \infty$. The boundary at $x = W_2$, which also extends
 378 to $\pm\infty$ in the y direction, is rigid and stress is not transmitted
 379 between plates **II** and **III**.

380 The equations of both elasticity and isostaticity are linear,
 381 given the respective constitutive properties, and it is sufficient
 382 to consider a point loading applied to the leftmost plate at the
 383 origin, $\bar{\sigma}(x = 0, y = 0)$. A more general loading is the super-
 384 position of such point loadings. The full solution to the point
 385 loading problem is detailed in the Supplemental Material [16].
 386 To summarize it, the stress field response in the marginally
 387 stable region **I**, whose example structure tensor is chosen to
 388 be uniform, for simplicity, $\bar{M} = \begin{pmatrix} 3 & 1 \\ 1 & -1 \end{pmatrix}$, consists of a finite
 389 stress only along two straight stress chains. The gradients of
 390 the stress chains are $\lambda_1 = 3$ and $\lambda_2 = -1$, and they follow
 391 the *characteristic* paths. Along each path, the stress field is
 392 a characteristic combination of the stress components that
 393 originate from the source at $(x = 0, y = 0)$. Outside these
 394 paths, the stress is exactly zero. This solution superposed with
 395 the uniform stress field due to the uniform loading on the
 396 boundary, which is also detailed in the Supplemental Material
 397 [16],

$$\bar{\sigma}_{\text{uniform}} = \begin{pmatrix} \sigma_{xx} & \sigma_{xy} \\ \sigma_{xy} & \sigma_{yy} = 3\sigma_{xx} + 2\sigma_{xy} \end{pmatrix}. \quad (7)$$

398 The value of the loading σ_{yy} must depend on the values of σ_{xx}
 399 and σ_{xy} to satisfy the constitutive stress-structure relation (6).

400 The stress chains of the solution are incident on the bound-
 401 ary between regions **I** and **II**, $x = W_1$, giving rise to two point

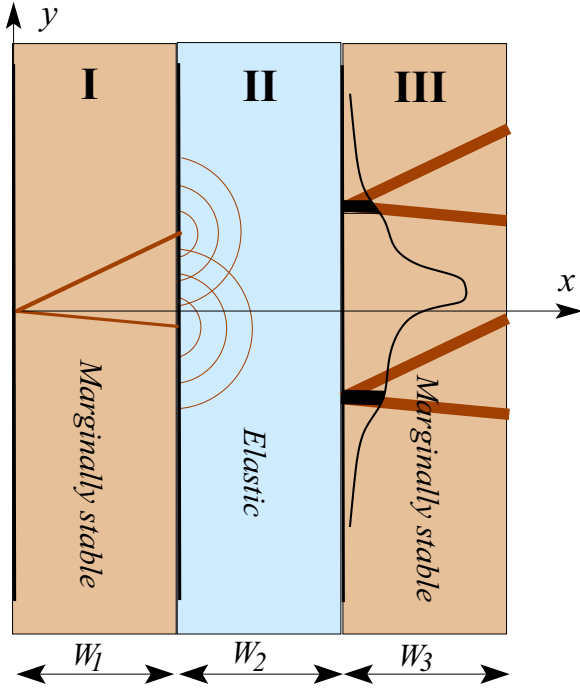


FIG. 1. A stack of alternating marginally stable and elastic plates. A localized stress is applied at the boundary $x = 0$, generating two stress chains that “propagate” along two characteristic paths. The chain stresses apply two localized loads on on the strain-free boundary at $x = W_1$. The boundary at $x = W_1$ deforms to transmit this stress to the elastic plate. The stress response within the elastic plate satisfies the elliptic equations of elasticity theory. The stress response on the strain-free boundary at $x = W_2$ is sketched. Adding another plate of marginally stable medium at $x = W_1 + W_2$, the stress solution within it is a superposition of the stress chains, which emanate from every point along this boundary, such as the two exemplified in the figure.

402 loadings on this boundary at $y = -W_1$ and $y = 3W_1$,

$$\begin{aligned} \bar{\sigma}_1(W_1, 3W_1) &= \frac{\sigma_{xx} + \sigma_{xy}}{4} \begin{pmatrix} 1 & 3 \\ 3 & 9 \end{pmatrix}, \\ \bar{\sigma}_2(W_1, -W_1) &= \frac{3\sigma_{xx} - \sigma_{xy}}{4} \begin{pmatrix} 1 & -1 \\ -1 & 1 \end{pmatrix}. \end{aligned} \quad (8)$$

403 The boundary condition at $x = W_1$ must be considered
 404 carefully now. If this boundary is presumed to remain straight
 405 and independent of y , then the stresses at the points $y =$
 406 $-W_1, 3W_1$ along this boundary would not be transmitted to the
 407 elastic medium. Some boundary deformation is required for
 408 that. The problem is that isostaticity theory does not provide a
 409 way to predict this deformation because strain plays no role
 410 in it. Nevertheless, such a deformation will occur because
 411 the application of the load at $(0,0)$ changes the structure
 412 wherever the stress is finite. This issue and its effect on the
 413 choice of this boundary condition are discussed in some detail
 414 in the concluding section, a discussion that touches on the
 415 assumptions underlying isostaticity theory. To summarize it
 416 here, since there is currently no theory to predict local struc-
 417 tural changes as a function of the local stress perturbation,
 418 the only way forward is to impose a boundary condition at

419 $x = W_1$ that transmits faithfully the stress from left to right.
 420 The natural way to achieve that is to impose a deformation,
 421 or strain, $\bar{\epsilon}$, that satisfies the stress-strain relation in the elastic
 422 medium, namely, $\bar{\sigma}(x = W_1^-, y) = \check{C}_{II}\bar{\epsilon}(x = W_1^+, y)$, with \check{C}_{II}
 423 the fourth-order stiffness tensor of the elastic medium in **II**.
 424 Applying this boundary condition to the problem at hand, the
 425 stress at the left boundary of plate **II** comprises two δ func-
 426 tions, as sketched in Fig. 1, and, together with the condition
 427 of a flat rigid boundary on the right of region **II**, make for a
 428 well-defined formulation for the solution in the elastic plate.

429 Since the strain at, and therefore the distortion to, the left
 430 boundary is known, a convenient way to solve for the stress
 431 in this region is to first mapping conformally the physical
 432 domain with the distorted boundary to a rectangle. Solve for
 433 the stress in the mapped domain, using textbook methods [41],
 434 and then transform the solution back to the physical plane.
 435 Two such point-loading solutions are sketched in the figure.

436 For completeness, it should be commented that, when the
 437 fabric tensor \bar{M} is not uniform in the marginally stable plate,
 438 secondary paths of lower stresses emanate from the main
 439 characteristic paths, which reach the boundary at $x = W_1$ at
 440 different locations. These modify the boundary stress for the
 441 elastic plate in a manner that can also be calculated from the
 442 solution in the Supplemental Material [16] and can be treated
 443 as a superposition of source points at $x = W_1$.

B. A chain of alternating-phase plates

444
 445 Next, consider a longer chain of parallel plate of alternat-
 446 ing phases, by adding them to the right of plates **I** and **II**.
 447 The first of this chain, **III**, is shown in Fig. 1. They have
 448 different thicknesses and all similarly extend to $\pm\infty$ in the
 449 y direction. Applying the same source load at $(x = 0, y =$
 450 $0)$, the stress response in plate **I** as well as its transmission
 451 across the boundary at $x = W_1$ are the same as for the pair
 452 system discussed above. The boundary condition at $x = W_2$
 453 is straightforward to determine: since the marginally stable
 454 medium in plate **III** is rigid, it is chosen to be flat. Then
 455 the solution in **II** is the same as in the pair system and,
 456 consequently, so is the stress at $\bar{\sigma}(x = W_2^-, y)$. This boundary
 457 stress is transmitted to the medium in **III** at $\bar{\sigma}(x = W_2^+, y)$.
 458 Assuming that the fabric tensor in **III** is the same as in **I**,
 459 the conceptual “propagation” from two arbitrary source points
 460 along the boundary at $x = W_2$ is exemplified in Fig. 1. Each
 461 such point plays the same role as the point load at $(x = 0, y =$
 462 $0)$.

463 A consistent set of boundary conditions for a chain of
 464 $2N$ such plates is then the following. The boundaries at
 465 $x = W_{2k}$ ($k = 1, 2, \dots, N/2$), which transmit stress from the
 466 $2k$ th elastic plate to the $(2k + 1)$ th marginally stable one, are
 467 presumed rigid and flat, while the boundaries at $x = W_{2k-1}$,
 468 which transmit stress from $(2k - 1)$ th marginally stable plate
 469 to the $2k$ th elastic one, deform such that the strain generated
 470 by the deformation matches the stress-strain relations in the
 471 elastic part, $\bar{\sigma}(x = W_1^-, y) = \check{C}_{2k}\bar{\epsilon}(x = W_1^+, y)$.

C. Effective medium method: Possibilities and difficulties

472
 473 The aim of this subsection is to outline an effective medium
 474 approximation (EMA) approach for deriving the stress in a

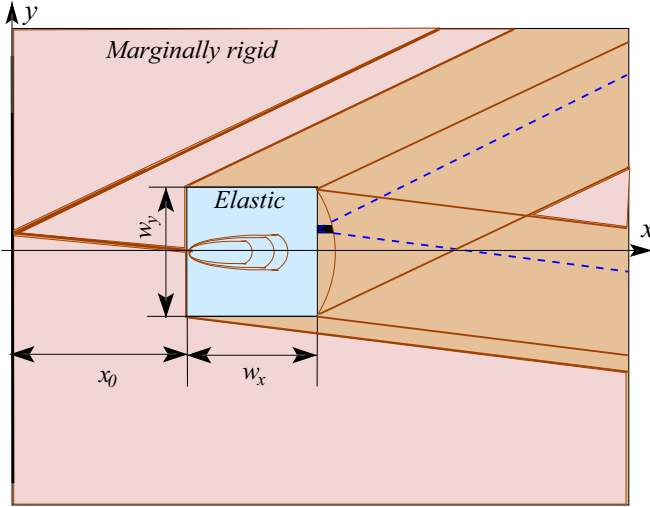


FIG. 2. A rectangular inclusion (light blue) in an otherwise marginally stable medium (light brown). Stress chains (dark brown) emanate from the point loading at $(0,0)$ along two narrow characteristic paths. The chain incident on the elastic inclusion deforms the boundary slightly, “letting” the stress through and giving rise to an intra-inclusion stress field that satisfies the linear elasticity equations. The inclusion’s other boundaries are rigid. The inclusion “diffracts” the stress, which reemerges into the marginally stable medium at a much attenuated magnitude along wider paths (dark brown regions).

475 general GM composite, rather than develop it in full detail.
 476 EMAs are based on the assumption that one phase is suf-
 477 ficiently dilute, often as inclusions, within the other. In this
 478 approximation, one neglects the effect of the inclusions on one
 479 another. Consequently, the key ingredient in an EMA is then
 480 the solution for an isolated inclusion of one phase within an
 481 otherwise much larger medium composed of the other phase.
 482 By interchanging the roles of the phases, this approach can
 483 be applied close to either the marginally stable state or the
 484 purely elastic state. Analysis of a marginally stable inclusion
 485 in an elastic medium is straightforward: the marginally stable
 486 medium can be regarded as a rigid inclusion in a large elas-
 487 tic medium, for which solutions exist or can be found with
 488 standard elasticity theory [42].

489 The opposite limit, of an elastic inclusion in a marginally
 490 stable medium, requires a careful consideration. While
 491 diffraction of hyperbolic characteristics from scatterers has
 492 been discussed in the literature [43], this is less relevant in this
 493 context than the stress developing within a finite inclusion. Let
 494 the medium occupy the half-space $x > 0$ and $-\infty < y < \infty$
 495 and the stiffness tensor within the inclusion be \check{C}_{inc} . For clar-
 496 ity, assume again that its fabric tensor is spatially uniform;
 497 as mentioned, position-dependent fabric tensors, $\check{\nabla} \cdot \check{M} \neq 0$,
 498 lead to nonstraight chains, stress attenuation along them, and
 499 branching, all of which, although making the treatment more
 500 involved quantitatively, can be included without any concep-
 501 tual difficulty in the following approach. It is convenient to
 502 consider a rectangular elastic inclusion, as shown in Fig. 2.

503 Consider a set of discrete point loadings on the boundary
 504 at $x = 0$, at intervals χ_i , with χ_i narrowly distributed around
 505 a mean value χ_0 . These act as sources, and from each one

506 can trace two characteristic paths into the marginally stable
 507 medium. The paths from one such source are shown in Fig. 2.
 508 The characteristic stress component combination on each path
 509 is determined by the solution described in the Supplemental
 510 Material [16]. In the absence of the inclusion, the stress field
 511 inside the medium, $\Sigma_0(x, y)$, consists of a network of stress
 512 chains. This solution would be unaffected when no chain is
 513 incident on the inclusion and the probability for this to happen,
 514 p_0 , decreases with W_y/χ_0 , most likely as e^{-W_y/χ_0} although its
 515 exact functional form is immaterial for the present discussion.

516 When a stress chain is incident on the inclusion, which
 517 is the case illustrated in Fig. 2, it provides a point load-
 518 ing on the boundary of the elastic inclusion at $x = x_0^-$. As
 519 illustrated in the alternating plates system, the way to trans-
 520 mit the stress to within the inclusion is by posing that this
 521 boundary is deformed into the inclusion such that the strain at
 522 $x = x_0^+$ satisfies $\bar{\sigma}(x = x_0^-, y = 0) = \check{C}_{\text{inc}} \bar{e}(x = x_0^+, y = 0) =$
 523 $\bar{\sigma}(x = x_0^+, y = 0)$. Following the example of the system of
 524 alternating plates, the boundaries of the inclusion, on which
 525 no stress chain is incident, should be regraded as flat and rigid.
 526 Given these conditions, the stress field inside the inclusion can
 527 be calculated either analytically or numerically, using linear
 528 elasticity. Again, if the calculation with the deformed bound-
 529 ary is problematic, one can conformally map the inclusion
 530 back to the original rectangle, solve for the intra-inclusion
 531 stress in the mapped plane, and then conformally map this
 532 solution back to the physical plane. A schematic illustration
 533 of contours of equal $\bar{\sigma}_{xx}$ within the inclusion is also shown
 534 in Fig. 2. This calculation then yields the stress distribution
 535 along the rigid boundaries, which are then transmitted to the
 536 rest of the marginally stable medium. This transmission must
 537 follow also the characteristic paths, as sketched in the figure.
 538 The “reemerging” stress paths are broad, corresponding to the
 539 size of the inclusion and orientation differences between the
 540 boundaries and the two characteristics.

541 As a consequence of force balance, the stress component
 542 magnitudes within the widened stress paths are suppressed
 543 to well below those of the original incident chain. Setting a
 544 detectability threshold, as for force chains, the stress is likely
 545 to drop below the threshold, and, to all practical purposes, the
 546 incident stress chain effectively terminates at the inclusion.
 547 The larger the inclusion, the wider the reemerging paths and
 548 the stronger the suppression. Denoting the single-inclusion
 549 stress field Σ_1 , the EMA stress field is

$$\Sigma_{\text{EMA}} = p_0 \Sigma_0 + (1 - p_0) \Sigma_1. \quad (9)$$

550 Placing a second inclusion elsewhere gives rise to a similar
 551 solution, Σ_2 . Since the inclusions are too far to interact, the
 552 EMA stress field due to n such inclusions is

$$\Sigma_{\text{EMA}} = p_0^n \Sigma_0 + (1 - p_0^n) \sum_{j=1}^n \Sigma_j(\vec{r} - \vec{r}_j), \quad (10)$$

553 in which \vec{r}_j denotes the position of the j th inclusion. Increas-
 554 ing the concentration of inclusions and/or their sizes, but
 555 without violating the effective medium assumption, increases
 556 the MCN, $z_c \rightarrow z = z_c + \delta z$. An increase in the inclusion
 557 concentration also increases the probability of incidence of
 558 stress chains on them and effectively terminating. The con-
 559 sequent shortening of the typical length of stress chains with

560 increase of the MCN is indeed consistent with experimental
 561 observations [44,45]. This also makes the EMA consistent
 562 with the idea that the value of δz controls the response length
 563 near the marginally stable critical point. Using then δz as a
 564 measure of the proximity to the critical point, it is tempting
 565 to conjecture that the relation between the stress chain typical
 566 length, \mathcal{L}_σ , and the “distance” from the critical point follows
 567 the conventional power-law form:

$$\mathcal{L}_\sigma \sim \delta z^{-\nu}; \quad \nu > 0. \quad (11)$$

568 This form is consistent with experimental observations near
 569 the marginal stability point [46], but it depends on more than
 570 the typical length of stress chains. This is because nonuniform
 571 fabric tensors, in which $\bar{\nabla} m_{ij} \neq 0$, give rise to coupled char-
 572 acteristics ω_i , which may lead to chains dropping below the
 573 threshold and terminating even if without incidence on inclu-
 574 sions [23,24]. These effects are not taken into consideration in
 575 (11), and to include them requires quantifying the dependence
 576 of this relation on the gradients of the fabric tensor \bar{M} . Strong
 577 gradients could not only lower the prefactor in (11) but also
 578 increase ν , with each of these effects suppressing \mathcal{L}_σ for a
 579 given δz . A full discussion of the effects of structure tensor
 580 inhomogeneity is beyond the scope of this work, but it offers
 581 an interesting line of future investigation.

582 VI. IDENTIFYING THE PHASES 583 IN THE TWO-PHASE COMPOSITES

584 To implement the two-phase-composite idea, it is impor-
 585 tant to have a clear way to identify the boundaries between the
 586 phases. This is particularly important in view of the required
 587 careful treatment of the boundary conditions. Unlike in many
 588 traditional two-phase composites, such an identification is not
 589 straightforward because the phases are visually very similar.
 590 The only structural difference between the phases is their con-
 591 nectivities per particle or specific connectivities. The specific
 592 connectivity of a region Γ is defined as $\delta z_\Gamma = z_\Gamma - z_{c,\Gamma}$, with
 593 $z_{c,\Gamma}$ the critical value of the MCN that makes the region Γ
 594 marginally stable and z_Γ the actual MCN of the particles
 595 within Γ . This value is different from that of the infinitely
 596 large assembly, calculated in Sec. II, due to the boundary
 597 corrections, which are no longer negligible.

598 A sketch of a finite domain, Γ , is shown in Fig. 3. It
 599 contains \mathcal{N}_Γ particles, of which \mathcal{N}_S are regarded as its surface
 600 and the boundary, $\partial\Gamma$ (dark brown in the figure), between
 601 Γ and the rest of the assembly. Let us define a stability pa-
 602 rameter as the difference between the number of unknown
 603 force components to determine and balance conditions, per
 604 particle in Γ ,

$$J_\Gamma \equiv \frac{(N_{\text{unknowns}})_\Gamma - (N_{\text{conditions}})_\Gamma}{\mathcal{N}_\Gamma}. \quad (12)$$

605 Dropping the subscript Γ , for brevity, the region is unstable
 606 and fluid when $J < 0$, marginally stable when $J = 0$, and
 607 stable and solid when $J > 0$. The specific connectivity and the
 608 stability parameter are equivalent for determining the phase
 609 because the number of unknowns is proportional to the num-
 610 ber of contacts. The calculation of the stability parameter of Γ
 611 is done as follows.

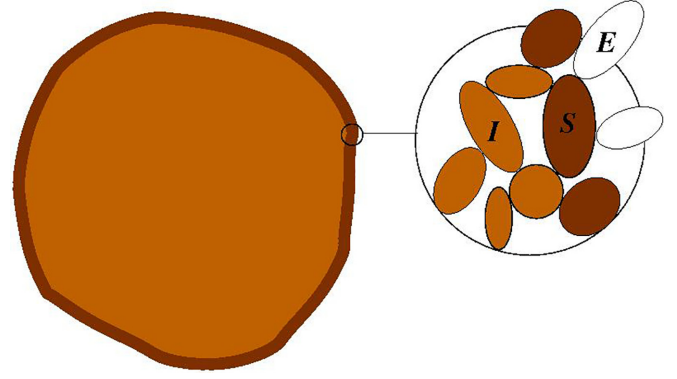


FIG. 3. A finite domain Γ within a larger granular assembly. The internal particles (light brown, particles labeled ‘I’) are surrounded by a surface (dark brown, particles labeled ‘S’), regarded as its boundary, $\partial\Gamma$, whose particles are in contact with external particles (white, particles labeled ‘E’).

612 Within Γ , there are C_{II} contacts between internal particles,
 613 C_{IS} contacts between internal and surface particles, and C_{SE}
 614 contacts between surface and external particles. The external
 615 particles exert forces on Γ through $\alpha\mathcal{N}_S$ contacts with the
 616 surface particles, with $\alpha = O(1)$. The premise is that all these
 617 quantities can be extracted visually from Γ . In the following,
 618 I focus on two-dimensional systems, for simplicity, but the
 619 analysis can be readily extended to three dimensions. The
 620 stability threshold depends on the particle surface friction and
 621 whether they are spheres or not. These are discussed next case
 622 by case.

623 A. Frictional particles in $d = 2$

624 In the calculation of the MCN of Γ , the contacts of the
 625 internal particles are counted twice each, while the contacts
 626 of the boundary particles with external particles are counted
 627 only once. This yields

$$z = \frac{2C_{II} + 2C_{IS} + C_{SE}}{\mathcal{N}}. \quad (13)$$

628 The forces at the C_{SE} contacts comprise the external loading
 629 on Γ and are regarded as known boundary loading for the
 630 purpose of determining the intra- Γ forces. These boundary
 631 forces are also presumed to be balanced (otherwise the as-
 632 sembly would not be static). The contacts C_{II} and C_{IS} transmit
 633 two force components each, giving $2(C_{II} + C_{IS})$ unknowns to
 634 resolve within Γ . These are to be compared to the $3\mathcal{N}$ balance
 635 conditions. Defining $p_S \equiv \mathcal{N}_S/\mathcal{N}$, we then have

$$\begin{aligned} J_A &= \frac{1}{\mathcal{N}}[2(C_{II} + C_{IS}) - 3\mathcal{N}] \\ &= z - 3 - \frac{C_{SE}}{\mathcal{N}}\mathcal{N} \\ &= z - 3 - \alpha p_S, \end{aligned} \quad (14)$$

636 corresponding to the critical point shifting to

$$z_{c,A} = 3 + \alpha p_S. \quad (15)$$

B. Frictionless nondisks in $d = 2$

Using the same definitions as above, the number of equations is the same, $3N$, but only the force magnitudes at the internal contacts are unknown, $C_{II} + C_{IS}$. Then

$$\begin{aligned} J_B &= \frac{1}{\mathcal{N}}[(C_{II} + C_{IS}) - (3\mathcal{N})] \\ &= \frac{z}{2} - \frac{C_{SE}}{2\mathcal{N}} - 3 \\ &= \frac{z}{2} - 3 - \frac{\alpha}{2}p_S. \end{aligned} \tag{16}$$

The critical point in this case is at

$$z_{c,B} = 6 + \alpha p_S. \tag{17}$$

C. Frictionless disks in $d = 2$

The number of unknowns is the same as in case B, but all the torque balance conditions are redundant, leaving only $2\mathcal{N}$ available equations. Therefore,

$$\begin{aligned} J_C &= \frac{1}{\mathcal{N}}[(C_{II} + C_{IS}) - 2\mathcal{N}] \\ &= \frac{z}{2} - \frac{C_{SE}}{2\mathcal{N}} - 2 \\ &= \frac{z}{2} - 2 - \frac{\alpha}{2}p_S. \end{aligned} \tag{18}$$

The critical point in this case is at

$$z_{c,C} = 4 + \alpha p_S. \tag{19}$$

Thus, in all three cases, the change to the infinite critical value is by adding αp_S .

The stability parameter J can be used to define a phase field parameter in mechanically stable granular assemblies, $\Psi \equiv 1 - H(J)$, with H the Heavyside step function. Ψ is unity in the marginally stable phase and vanishes in the overconnected phase. It can be used to develop phase-field simulations, in which it would determine the stress equations to use and where phase boundaries are. It is straightforward to extend the calculations of J to three and higher dimensions, using the same rationale.

VII. CONCLUSION

To conclude, this paper should be regarded as a step toward a continuum stress theory of general mechanically stable GM, which goes beyond marginally stable states and the yield surface. The proposition is that real systems should be regarded as comprising two phases: one marginally stable and the other overconnected. The conditions for marginal stability in large assemblies in arbitrary dimensionality and the first-principles formulation of isostaticity theory, including the explicit solutions to the stress field equations in $d = 2$, have been reviewed briefly. A thought experiment was described which supports strongly the feasibility of the two-phase picture. In particular, it showed that there is a continuous spectrum of system structures that extends from the marginally stable state, through a general granular assembly and a porous medium, to a continuum uniform solid. To highlight the issues involved in deriving stress fields in two-phase systems, the problem

was solved for a simple case: a stack of plates of alternating phase. This problem also highlighted the constraints on the boundary conditions. The critical-point-like nature of the marginally stable state has been used to extend the theory near this state. Specifically, a variation of the effective medium approximation (EMA) has been formulated for this problem and analyzed. Finally, a quantitative stability parameter has been defined, which helps with the difficult problem of identifying the different phases and their boundaries within a given granular assembly. This parameter can be used for developing phase-field approaches to the problem.

Several points are worth discussing. One is the effects of gradients of $\overline{\overline{M}}$ on the stress chains typical length in the EMA method. The criticality of the marginally stable state is because a small local displacement of a particle is likely to break a contact, which destabilizes the local structure by definition. This leads to local rearrangement, which causes another contact to break and so on. The long-range rearrangement due to a small local perturbation is the analog of a diverging response length near traditional critical points. While it is tempting to relate the rearrangement response to the stress and, in particular, to the typical length of stress chains, this relation holds only in media with relatively uniform fabric tensors, $\overline{\overline{M}}$. This is because, as mentioned in Sec. V, spatial gradients of m_{ij} give rise to secondary chains that split from the main chains and siphon stress away from them. Consequently, the stress attenuates along the main chain. The rate of this attenuation depends on the gradients magnitude along the chain, and once the stress drops below some observability threshold, chains effectively terminate even though the medium is still ideally marginally stable and the rearrangement response is still very long range. This is another manifestation of the decoupling between the stress and the strain in marginally stable media.

Another consideration enters this picture: isostaticity is a continuum theory, and the EMA method requires an elementary volume over which the structure tensor is coarse grained. This has two effects. One is that the gradients are milder on the coarse-grained scale, and the other, that stress chains cannot be thinner than the linear size of an elementary volume. Both these effects counteract the shortening of the response length and must also be taken into account in structurally inhomogeneous systems. An investigation into this issue must also be part of the further development of the general stress theory.

Another subtle issue is the following. In the solution for the uniform stress, (7), whose full derivation is in the Supplemental Material [16], the σ_{yy} component of the boundary stress was taken to satisfy the stress-structure relation imposed by the local structure tensor, $\overline{\overline{M}} : \overline{\overline{\sigma}} = 0$, and it is therefore a local function of σ_{xx} and σ_{xy} . This may seem strange because one expects to be able to choose all the components of the boundary stress at will. However, there is no inconsistency! It has been shown that structure and the stress self-organize cooperatively [47–49], namely, one cannot change without a corresponding change to the other. Self-organization is a fundamental phenomenon GM, at least if the settling follows quasistatic dynamics. Thus, choosing a different value of σ_{yy} at some point on the boundary should have the effect of restructuring the contact network near that point, and that

734 restructuring perturbation would propagate into the system as
 735 far as the stress response length. Such a self-organization has
 736 been discussed and quantified to some extent in the literature
 737 [47,48,50]. Yet there is no theory to predict the resultant mod-
 738 ified structure tensor due to an arbitrary stress perturbation.
 739 It is likely that the structure would be most strongly modifi-
 740 fied close to the source of perturbation and unaffected very
 741 far from it, which means that gradients must develop. Once
 742 the structure has rearranged and the new structure tensor is
 743 known, the derivation of the stress field in the GM follows
 744 the same procedure that led to Eq. (7), albeit with coupling
 745 between the characteristics. Moreover, it is the inability to
 746 predict the structural response in marginally stable media to
 747 stress perturbations which necessitated the tailoring of the
 748 boundary conditions to describe stress transmission from a
 749 marginally stable to elastic medium.

750 While the discussion in this paper focused on two phases
 751 in static GM, it is interesting to note that two phases have also
 752 been discussed in the context of dense granular flows: plug re-
 753 gions, which are clusters of particles moving rigidly together,
 754 and plug-free regions, in which the velocity gradients are finite
 755 [51–53]. It is possible that, upon settling, the plug regions have

756 a higher tendency to become the overconnected regions. This
 757 conjecture can be tested by measuring the correlation between
 758 a presettling particle belonging to a plug and its postsettling
 759 belonging to an overconnected particle.

760 Finally, there remain several hurdles in implementing this
 761 theory in practical modeling of natural systems and engineer-
 762 ing applications. These include, but are probably not limited
 763 to, effective modeling of the constitutive fabric tensor $\overline{\mathbf{M}}$ on
 764 relevant length scales and determining the relative concentra-
 765 tions of the two phases. More work is needed to address these
 766 issues. However, the reward of such work cannot be overem-
 767 phasized because a first-principles theory of real GM outside
 768 the yield surface has the potential to improve significantly
 769 predictability of models in a range of engineering disciplines.

770 Data sharing not applicable to this article as no
 771 data sets were generated or analyzed during the current
 772 study [54,55].

ACKNOWLEDGMENTS

773 This research did not receive any specific funding. The
 774 author declares that he has no competing interests to report.
 775

-
- [1] Archimedes, *The Sand Reckoner* (ca. 3rd century BCE), in
The Works of Archimedes, edited by T. L. Heath (Cambridge
 University Press, UK, 2009).
- [2] O. Reynolds, *Phil. Mag. Series 5*, **20**, 469 (1885).
- [3] R. A. Bagnold, *The Physics of Blown Sand and Desert Dunes*
 (Methuen, London, 1941).
- [4] S. F. Edwards and R. B. Oakeshott, *Physica D* **38**, 88 (1989).
- [5] S. F. Edwards and R. B. Oakeshott, *Physica A* **157**, 1080 (1989).
- [6] A. Mehta and S. F. Edwards, *Physica A* **157**, 1091 (1989).
- [7] R. P. Seelig and J. Wulff, *Trans. AIME* **166**, 492 (1946).
- [8] T. Wakabayashi, *Proc. 7th Jpn. Nat. Cong. Appl. Mech.*, 153
 (1957).
- [9] P. Dantu, *Proc. 4th Int. Conf. Soil Mech. and Found. Eng.*, 144
 (1957).
- [10] D. F. Bagster and R. Kirk, *J. Powder Bulk Solids Technol.* **1**, 19
 (1985).
- [11] D. Howell and R. P. Behringer, in *Powders and Grains 97*,
 edited by R. P. Behringer and J. T. Jenkins (Balkema, Rotter-
 dam, 1997), p. 337.
- [12] M. Oda and H. Kazama, *Géotechnique* **48**, 465 (1998).
- [13] L. Vanel, D. Howell, D. Clark, R. P. Behringer, and E. Clement,
Phys. Rev. E **60**, R5040(R) (1999).
- [14] T. S. Majmudar, M. Sperl, S. Luding, and R. P. Behringer, *Phys.*
Rev. Lett. **98**, 058001 (2007).
- [15] R. Blumenfeld, *Phys. Rev. Lett.* **93**, 108301 (2004).
- [16] See Supplemental Material at [http://link.aps.org/supplemental/
 10.1103/PhysRevE.xx.xxxxx](http://link.aps.org/supplemental/10.1103/PhysRevE.xx.xxxxx) for the general solution of the
 isostaticity equations in $d = 2$ and the solution of the isostatic-
 ity equations for the uniform boundary loading, which include
 Refs. [54,55].
- [17] N. I. Muskhelishvili, *Some Basic Problems of the Mathematical
 Theory of Elasticity* (Noordhoff, Groningen, 1963).
- [18] J. P. Wittmer, P. Claudin, M. E. Cates, and J.-P. Bouchaud,
Nature (London) **382**, 336 (1996).
- [19] J. P. Wittmer, M. E. Cates, and P. Claudin, *J. Phys. I (France)* **7**,
 39 (1997).
- [20] M. E. Cates, J. P. Wittmer, J.-P. Bouchaud, and P. Claudin, *Phys.*
Rev. Lett. **81**, 1841 (1998).
- [21] M. E. Cates, J. P. Wittmer, J.-P. Bouchaud, and P. Claudin, *Phil.*
Trans. Roy. Soc. A, **356**, 2535 (1998).
- [22] R. C. Ball and R. Blumenfeld, *Phys. Rev. Lett.* **88**, 115505
 (2002).
- [23] M. Gerritsen, G. Kreiss, and R. Blumenfeld, *Phys. Rev. Lett.*
101, 098001 (2008).
- [24] R. Blumenfeld and J. Ma, *Granular Matter* **19**, 29 (2017).
- [25] See, e.g., J. C. Jaeger and N. G. W. Cook, *Fundamentals of Rock
 Mechanics*, 3rd ed. (Chapman & Hall, London 1979).
- [26] H. Tresca, *C. R. Hebd. Acad. Sci.* **59**, 754 (1864).
- [27] R. von Mises, *Nachr. Ges. Wiss. Goett. Math. Kl.* **1**, 582 (1913).
- [28] D. C. Drucker and W. Prager, *Q. Appl. Math.* **10**, 157 (1952).
- [29] R. Blumenfeld, in *IMA Volume in Mathematics and its Ap-
 plications*, edited by M.-C. T. Calderer and E. M. Terentjev,
 Modeling of Soft Matter (Springer-Verlag, 2005), Vol. 141, pp.
 235–246.
- [30] J. Ren, J. A. Dijksman, and R. P. Behringer, *Phys. Rev. Lett.*
110, 018302 (2013).
- [31] G. Düring, E. Lerner, and M. Wyart, *Phys. Rev. E* **89**, 022305
 (2014).
- [32] E. DeGiuli, A. Laversanne-Finot, G. Düring, E. Lerner, and M.
 Wyart, *Soft Matter* **10**, 5628 (2014).
- [33] T. S. Majmudar and R. P. Behringer, *Nature (London)* **435**, 1079
 (2005).
- [34] J. Zhang, T. S. Majmudar, and R. P. Behringer, *Chaos* **18**,
 041107 (2008).
- [35] J. Zhang, T. S. Majmudar, A. Tordesillas, and R. P. Behringer,
Granular Matter **12**, 159 (2010).
- [36] K. E. Daniels, J. E. Kollmer, and J. G. Puckett, *Rev. Sci.*
Instrum. **88**, 051808 (2017).

- [37] Y. Zhao, H. Zheng, D. Wang, M. Wang, and R. P. Behringer, *New J. Phys.* **21**, 023009 (2019).
- [38] R. J. Mora and A. M. Waas, *Proc. R. Soc. London A* **458**, 1695 (2002).
- [39] H. Laubie, F. Radjai, R. Pellenq, and F.-J. Ulm, *Phys. Rev. Lett.* **119**, 075501 (2017).
- [40] F. Radjai, D. E. Wolf, M. Jean, and J.-J. Moreau, *Phys. Rev. Lett.* **80**, 61 (1998).
- [41] N. I. Muskhelishvili, *Some Basic Problems of the Mathematical Theory of Elasticity* (Noordhoff, Groningen, 1963).
- [42] O. Mattei and M. Lim, *J. Elasticity* **144**, 81 (2021).
- [43] P. Claudin, J.-P. Bouchaud, M. E. Cates, and J. P. Wittmer, *Phys. Rev. E* **57**, 4441 (1998).
- [44] D. Howell, R. P. Behringer, and C. Veje, *Phys. Rev. Lett.* **82**, 5241 (1999).
- [45] R. P. Behringer and B. Chakraborty, *Rep. Prog. Phys.* **82**, 012601 (2019).
- [46] M. Wang, D. Wang, J. E. S. Socolar, H. Zheng and R. P. Behringer, *Granular Matter* **21**, 102 (2019).
- [47] T. Matsushima and R. Blumenfeld, *Phys. Rev. Lett.* **112**, 098003 (2014).
- [48] T. Matsushima and R. Blumenfeld, *Phys. Rev. E* **95**, 032905 (2017).
- [49] X. Jiang, R. Blumenfeld, and T. Matsushima, [arXiv:2208.06582](https://arxiv.org/abs/2208.06582) [cond-mat.soft].
- [50] R. Blumenfeld, S. F. Edwards and S. M. Walley, in *The Oxford Handbook of Soft Condensed Matter*, edited by E. M. Terentjev and D. A. Weitz (Oxford University Press, Oxford, 2015), p. 167.
- [51] R. Blumenfeld, S. F. Edwards, and M. Schwartz, *Eur. Phys. J. E* **32**, 333 (2010).
- [52] M. Schwartz and R. Blumenfeld, *Granular Matter* **13**, 241 (2011).
- [53] P. Kharel and P. Rognon, *Phys. Rev. Lett.* **119**, 178001 (2017).
- [54] R. Blumenfeld, *Granular Matter* **22**, 38 (2020).
- [55] M. Gerritsen, G. Kreiss, and R. Blumenfeld, *Physica A* **387**, 6263 (2008).